

Splitting methods for relaxation two-phase flow models

H. Lund^a, P. Aursand^b

^aDept. of Energy and Process Engineering, Norwegian University of Science and Technology (NTNU), NO-7491 Trondheim, Norway, halvor.lund@ntnu.no

^bSINTEF Energy Research, Sem Sælands vei 11, NO-7465 Trondheim, Norway

Abstract

A model for two-phase pipeline flow is presented, with evaporation and condensation modelled using a relaxation source term based on statistical rate theory. The model is solved numerically using a Godunov splitting scheme, making it possible to solve the hyperbolic fluid-mechanics equation system and the relaxation term separately. The hyperbolic equation system is solved using the multi-stage (MUSTA) finite volume scheme. The stiff relaxation term is solved using two approaches: One based on the Backward Euler method, and one using a time-asymptotic scheme. The results from these two methods are presented and compared for a CO₂ pipeline depressurization case.

Keywords: hyperbolic conservation laws; relaxation; splitting methods; phase transfer; exponential integrator

This paper is a revised and expanded version of a paper with the same title presented at the ECCOMAS Young Investigators conference, Aveiro 24-27 April, 2012.

Introduction

Two-phase flow is present in many industrial situations, such as heat exchangers, oil and gas production, CO₂ transport and storage, and in the nuclear industry. Modelling of such flows is known to be a challenging task, much due to the possibly complex behaviour of the interface in different flow regimes, and interaction between the phases occurring at this interface, for example heat or mass transfer or interface friction.

If the precise shape of the interface is of little interest or too computationally expensive to calculate, one can apply *averaging* of the physical quantities over a certain area or volume. This typically leads to systems of hyperbolic balance laws for mass, momentum and energy. Transfer of heat, mass and momentum between the two phases can then be modelled in the form of source terms in these balance equations. This paper will focus on the modelling and numerical solution of a mass transfer term which models evaporation and condensation between the liquid and gas phase. Evaporation of liquid in a pipeline will cause potentially large temperature drops, rendering the pipe steel brittle and vulnerable to rupture, and is therefore crucial to predict.

Relaxation source terms for mass may be stiff, i.e. the time scales associated with the relaxation process might be significantly shorter than those of the hyperbolic flux term in the fluid-dynamical model. A stiff source term requires careful numerical treatment to avoid instabilities. One method to accomplish this, is to use a fractional-step (or splitting) method, which divides the problem into two parts: The hyperbolic (homogeneous) conservation equations and the source term. These two parts can then be solved separately using methods well suited for each part.

The paper is organized as follows: The first section presents the models needed to describe the fluid-mechanical behaviour as well as the mass transfer. Then the numerical methods for solving these models are described, where the splitting procedure is outlined, followed by methods for solving the hyperbolic fluid-mechanical conservation laws and the mass transfer source term separately. Numerical results for a CO₂ pipeline depressurization case are presented, and the results for two different numerical methods are compared. Finally, the work is summarized and possible further work is outlined.

Models

To construct a model for two-phase flow with phase transfer, one needs a fluid-mechanical model, a model to describe the phase transfer, and a thermo-dynamic model or equation of state (EOS). In the following, each of these models will be presented.

Fluid-mechanical model

Fluid-mechanical models for two-phase flow are often averaged over a certain area or volume to reduce the computational cost and remove the need to explicitly model the location of the gas-liquid interface. Such averaged models are typically formulated as hyperbolic equation systems for mass, momentum and energy. In order to focus on the effect of the numerical solution of the phase transfer model, it is desirable to use a fluid-mechanical model which is as simple as possible. In this paper, a four-equation homogeneous flow model is chosen, with one mass balance (continuity) equation for each phase, together with equations for conservation of total momentum and energy,

$$\frac{\partial(\alpha_g \rho_g)}{\partial t} + \frac{\partial(\alpha_g \rho_g v)}{\partial x} = \Gamma, \quad (1)$$

$$\frac{\partial(\alpha_\ell \rho_\ell)}{\partial t} + \frac{\partial(\alpha_\ell \rho_\ell v)}{\partial x} = -\Gamma, \quad (2)$$

$$\frac{\partial(\rho v)}{\partial t} + \frac{\partial(\rho v^2 + p)}{\partial x} = 0, \quad (3)$$

$$\frac{\partial E}{\partial t} + \frac{\partial[(E + p)v]}{\partial x} = 0, \quad (4)$$

where α_k is the volume fraction and ρ_k is the density of phase k , where k is g (gas) or ℓ (liquid). The mixture density is $\rho = \alpha_g \rho_g + \alpha_\ell \rho_\ell$, and the mixture energy is $E = \alpha_g \rho_g e_g + \alpha_\ell \rho_\ell e_\ell + \frac{1}{2} \rho v^2$, where e_k is the internal energy of phase k . This model could be argued to be the simplest possible pipe flow model which still incorporates a phase-transfer term. Flåtten et al. (2010) (among others) have analyzed this model in the frozen-phase limit $\Gamma = 0$. To close the model, it is assumed that the two phases have equal pressures p , temperatures T and velocities v . The phase transfer appears as a source term, Γ , in the mass balance equations (1)–(2).

Phase transfer model

Modelling phase transfer between gas and liquid can be done using a variety of different approaches, and there does not seem to exist a universally correct one. Among the most common are kinetic theory, non-equilibrium (irreversible) thermodynamics and statistical rate theory (SRT). The latter is a rather newly suggested approach based on statistical mechanics, and was first introduced by Ward et al. (1982) and later applied to modelling of liquid evaporation (Ward & Fang, 1999). One of the main reasons for the development of SRT was to be able to explain the anomalous temperature profiles found close to an evaporation interface (Pao, 1971). Statistical rate theory assumes that interfacial transport processes, on a microscopical level, are caused by single molecular events. The probability of each event is calculated using a first-order perturbation analysis of the Schrödinger equation, together with the Boltzmann definition of entropy. Since its introduction by Ward et al. (1982), SRT has been used to model a number of different transport processes, including crystal growth (Dejmek & Ward, 1998), solution/solid adsorption (Azizian et al., 2008; Rudzinski & Plazinski, 2006), gas/solid adsorption (Elliott & Ward, 1997a; Findlay & Ward, 1982), temperature programmed desorption (Elliott & Ward, 1997b), ion permeation across lipid membranes (Bordi et al., 2000), chemical reactions (Harding et al., 2000), and evaporation and condensation (Ward & Fang, 1999; Kapoor & Elliott, 2008; Ward & Stanga, 2001).

Lund and Aursand (2012) developed an explicit expression for the phase transfer source term Γ in Eqs. (1)–(2) based on SRT, following an approach similar to that of Ward et al. (1982); Ward and Fang (1999). They found an interfacial flux per area expressed as

$$J = \rho_g \sqrt{\frac{k_B T}{2\pi m}} \left(\exp \left[\frac{m(\mu_\ell - \mu_g)}{k_B T} \right] - \exp \left[\frac{m(\mu_g - \mu_\ell)}{k_B T} \right] \right), \quad (5)$$

where m is the molecular mass and k_B the Boltzmann constant. The chemical potential per mass of phase k is denoted μ_k . This flux has the important property that it reduces to zero when the chemical potentials are equal, as expected. An advantage with the SRT approach, is that it is able to yield an explicit expression without any parameters that need tuning, as seen in Eq. (5). Other methods are often dependent on parameters which need to be empirically determined.

One also needs to approximate the interfacial area across which the flux J flows. Since the fluid-mechanical model is an averaged model, one has little information about the precise shape of the interface. Hence it is assumed that the flow is stratified-like, and that the interfacial area can be approximated by (Lund & Aursand, 2012)

$$A_{\text{int}} = \begin{cases} 4DL(\alpha_g + \delta)\alpha_\ell & \text{if } \mu_g < \mu_\ell, \\ 4DL\alpha_g(\alpha_\ell + \delta) & \text{if } \mu_g \geq \mu_\ell, \end{cases} \quad (6)$$

where D is the diameter of the pipe and L is the length of the interface in x -direction. The term δ is a tunable *initial volume fraction* which ensures that the evaporation or condensation can start even when the mass-receiving phase has zero volume fraction. To ensure that this term only has a small effect, it should be kept smaller than typical volume fraction values, so $\delta \ll 1$.

With the given flux (5) and interfacial area (6), one finds the following expression for the phase transfer source term in Eqs. (1)–(2) (Lund & Aursand, 2012):

$$\Gamma = \begin{cases} \frac{32\rho_g(\alpha_g + \delta)\alpha_\ell}{\pi D} \sqrt{\frac{m}{2\pi k_B T}} (\mu_\ell - \mu_g) & \text{if } \mu_g < \mu_\ell, \\ \frac{32\rho_g\alpha_g(\alpha_\ell + \delta)}{\pi D} \sqrt{\frac{m}{2\pi k_B T}} (\mu_\ell - \mu_g) & \text{if } \mu_\ell \leq \mu_g, \end{cases} \quad (7)$$

where the exponentials have been expanded to first order in $\mu_g - \mu_\ell$. This model has the advantage of having an explicit mathematical expression, as well as being based on well-established physics principles such as statistical mechanics. Models in a similar form, with the phase transfer rate proportional to the difference in chemical potential, have also been used by a number of other authors, including Saurel et al. (2008) and Stewart and Wendroff (1984).

Equation of state

In this paper, the stiffened gas equation of state (see e.g. Menikoff and Plohr (1989)) is used, which has the advantage of allowing analytical expressions for most thermodynamic relations, while still being sophisticated enough to give reasonable results for a certain range of pressures and temperatures. It can essentially be seen as an ideal gas with a stiffening term, p_∞ , which allows a non-zero density at zero pressure, making it suitable to model liquids as well as gases. The pressure, internal energy and chemical potential in a stiffened gas are given by

$$p(\rho, T) = \rho(\gamma - 1)c_v T - p_\infty, \quad (8)$$

$$e(\rho, T) = c_v T + \frac{p_\infty}{\rho} + e_*, \quad (9)$$

$$\mu(\rho, T) = \gamma c_v T + e_* - c_v T \ln\left(\frac{T}{T_0} \left(\frac{\rho_0}{\rho}\right)^{\gamma-1}\right) - s_0 T, \quad (10)$$

where γ is the ratio of specific heats, c_v is the heat capacity at constant volume and e_* is the zero point of energy. The reference temperature, density and entropy are denoted T_0 , ρ_0 and s_0 , respectively. Each phase has its own set of parameters, which can be fitted to experimental values.

Numerics

The fluid-mechanical equation system (1)–(4) can be compactly formulated as

$$\frac{\partial \mathbf{q}}{\partial t} + \frac{\partial \mathbf{f}(\mathbf{q})}{\partial x} = \mathbf{s}(\mathbf{q}), \quad (11)$$

where $\mathbf{q} = [\alpha_g \rho_g, \alpha_\ell \rho_\ell, \rho v, E]$, $\mathbf{f}(\mathbf{q})$ is the flux function and $\mathbf{s}(\mathbf{q})$ is the source term. There typically exist well-developed methods for solving homogeneous equation systems, i.e. with $\mathbf{s} = 0$. However, if the source term is stiff, problems relating to stability may arise. Therefore, Eq. (11) will be solved using a first-order fractional-step method known as Godunov splitting (LeVeque, 2002, Ch. 17). This advances the solution \mathbf{q}^n from time t_n to time $t_{n+1} = t_n + \Delta t$ using two steps:

1. Solve the hyperbolic homogeneous conservation law given by

$$\frac{\partial \mathbf{q}}{\partial t} + \frac{\partial \mathbf{f}(\mathbf{q})}{\partial x} = 0, \quad t \in [t_n, t_{n+1}], \quad \mathbf{q}(t_n) = \mathbf{q}^n, \quad (12)$$

yielding an intermediate solution \mathbf{q}^* .

2. Solve the ordinary differential equation given by

$$\frac{d\mathbf{q}}{dt} = \mathbf{s}(\mathbf{q}), \quad t \in [t_n, t_{n+1}], \quad \mathbf{q}(t_n) = \mathbf{q}^*, \quad (13)$$

giving the solution at time t_{n+1} .

This method will be first-order accurate in time as long as each of the two steps are at least first-order accurate in time. With such a fractional-step (splitting) scheme, one can employ efficient, accurate and stable numerical methods in each step, constructed specifically for each part of the problem.

Higher-order accurate fractional-step methods can be derived, an example being the second order Strang splitting (Strang, 1968). Schemes of even higher order exist, but are often subject to stability issues. Moreover, as shown by Jin (1995), higher order splitting schemes can reduce to first-order accuracy in the stiff limit.

In this work first-order splitting will be considered, and in the following methods for solving Eqs. (12)–(13) will be described.

Hyperbolic conservation law

As fluid-mechanical models typically are formulated as conservation laws, as is the case with Eq. (12), they are often solved using finite volume methods, which ensure that the physically conserved variables are also conserved numerically. By integrating Eq. (12) over a control volume i , one gets

$$\frac{dQ_i}{dt} = -\frac{1}{\Delta x}(\mathbf{F}_{i+1/2} - \mathbf{F}_{i-1/2}), \quad (14)$$

where Δx is the control volume size, Q_i is the average of the conserved variable q over control volume i , while $\mathbf{F}_{i+1/2}$ is the numerical flux between control volumes i and $i + 1$, which should approximate the exact flux at the interface,

$$\mathbf{F}_{i+1/2} \approx \mathbf{f}(q(x_{i+1/2}, t)). \quad (15)$$

As expected from a conserving scheme, the quantity Q_i is only changed due to fluxes in and out of the control volume. The challenge now lies in approximating the fluxes $\{\mathbf{F}_{i+1/2}\}$ at the control volume interfaces, knowing only the control volume averages $\{Q_i\}$. This can be visualized as a discontinuity in Q at each interface at time t_n , and solving for later times is known as solving a Riemann problem.

There exists a number of different finite volume schemes to calculate the numerical fluxes in Eq. (14), and one can, in general, divide these into two groups: upwind schemes and centred schemes. Upwind schemes have the advantage that they take into account how waves propagate in the original equation system, so that each cell is only affected by information in the cells from where the waves are coming, hence the term *upwind*. One of the most well-known schemes of this type is Roe's approximate Riemann solver (Roe, 1981). The centred schemes, on the other hand, have no concept of waves and treats information in both directions equally, hence the term *centred*.

Although the upwind schemes typically perform better for e.g. discontinuities, a centred scheme will be used in this paper, which has the advantage of being robust and easy to derive. The multi-stage (MUSTA) centred scheme was first proposed by Toro (2003), and is based on solving the Riemann problem at each interface by introducing a local grid and local time stepping. This method can be divided into the following three steps, which are also illustrated in Figure 1.

1. At each cell interface, define a local grid with $2N$ cells
2. Do M time steps in each local grid, using a first-order centred FORCE flux
3. Use the fluxes from the local grids as fluxes in the original grid

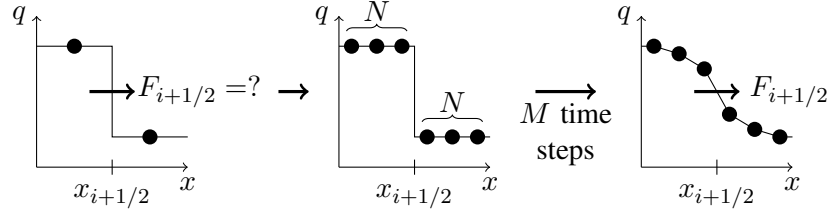


Figure 1. Illustration of the steps in the MUSTA method for *one* interface, between control volumes i and $i + 1$.

To calculate the fluxes in the local grid, a first-order centred scheme known as FORCE will be used. This flux is given by (Toro, 1999)

$$\mathbf{F}_{j+1/2}^{\text{FORCE}} = \frac{1}{2}(\mathbf{F}_{j+1/2}^{\text{LF}} + \mathbf{F}_{j+1/2}^{\text{Ri}}), \quad (16)$$

where $\mathbf{F}_{j+1/2}^{\text{LF}}$ is the Lax-Friedrichs flux

$$\mathbf{F}_{j+1/2}^{\text{LF}} = \frac{1}{2}(\mathbf{f}(\mathbf{Q}_j) + \mathbf{f}(\mathbf{Q}_{j+1})) - \frac{\Delta x}{2\Delta t}(\mathbf{Q}_{j+1} - \mathbf{Q}_j), \quad (17)$$

and $\mathbf{F}_{j+1/2}^{\text{Ri}}$ is the Richtmyer flux. It is computed by first defining an intermediate state

$$\mathbf{Q}_{j+1/2}^{\text{Ri}} = \frac{1}{2}(\mathbf{Q}_j + \mathbf{Q}_{j+1}) - \frac{\Delta t}{2\Delta x}(\mathbf{f}(\mathbf{Q}_{j+1}) - \mathbf{f}(\mathbf{Q}_j)), \quad (18)$$

and then setting the flux on the global grid to

$$\mathbf{F}_{j+1/2}^{\text{Ri}} = \mathbf{f}(\mathbf{Q}_{j+1/2}^{\text{Ri}}). \quad (19)$$

With the FORCE flux (16), one can then perform time steps on the local grid using a finite volume scheme in a form equivalent to Eq. (14). The time step used in the local grid is calculated using a *local* CFL criterion, given by

$$\Delta t_{\text{loc}} = \frac{C_{\text{loc}}\Delta x}{\max_{1 \leq j \leq 2N} \left(\max_{1 \leq p \leq d} |\lambda_j^p| \right)},$$

where $C_{\text{loc}} \in (0, 1)$ is the local CFL number. λ_j^p is the p th eigenvalue of the Jacobian $\partial_{\mathbf{q}} \mathbf{f}(\mathbf{q})$ at grid point j . The denominator is simply the largest absolute eigenvalue in the local grid.

Before each time step, extrapolation boundary conditions are applied, $\mathbf{Q}_0^m = \mathbf{Q}_1^m$ and $\mathbf{Q}_{2N+1}^m = \mathbf{Q}_{2N}^m$, where the superscript m denotes the m th time step. After the M th time step, one has found the flux to use in the global grid, namely $\mathbf{F}_{N+1/2}^M$. Summarized, the local time steps at each control volume interface are performed as follows (Titarev & Toro, 2005):

1. Compute fluxes using Eq. (16).
2. If $m = M$, then return flux $\mathbf{F}_{N+1/2}^M$ to be used in global grid.
3. Apply extrapolation boundary conditions: $\mathbf{Q}_0^m = \mathbf{Q}_1^m$ and $\mathbf{Q}_{2N+1}^m = \mathbf{Q}_{2N}^m$.
4. Update solution forward in time using a local finite volume scheme similar to Eq. (14), with the FORCE flux (16), for $j \in \{1, 2, \dots, 2N\}$.
5. Increase m and by one repeat from step 1.

In the numerical simulations presented in the numerical results section, a MUSTA 2-2 method ($M = N = 2$) will be used, with 4 local grid cells and 2 local time steps, similar to the one described by Munkejord et al. (2006).

Relaxation ODE

The second part of the splitting scheme concerns the relaxation term, formulated as the ODE

$$\frac{d\mathbf{q}}{dt} = \mathbf{s}(\mathbf{q}), \quad t \in [0, \Delta t], \quad \mathbf{q}(t=0) = \mathbf{q}^*. \quad (20)$$

When the time scales of the relaxation process (20) become significantly smaller than the time scales of the hyperbolic conservation law (12), one is dealing with a stiff relaxation system. For efficiency and simplicity, it is often of interest to resolve the solution at time scales comparable with those of the conservation law. However, doing so in a robust manner requires an ODE solver for Eq. (20) with good stability properties. In particular, there is a risk of *overshooting* the equilibrium point \mathbf{q}^{eq} defined by

$$\mathbf{s}(\mathbf{q}^{\text{eq}}) = 0, \quad (21)$$

in the ODE step of the fractional-step method, due to large time steps Δt .

Backward Euler. For first-order accuracy, an obvious choice for solving the system (20) is the implicit Backward Euler scheme, given by

$$\mathbf{q}^{n+1} = \mathbf{q}^* + \mathbf{s}(\mathbf{q}^{n+1}). \quad (22)$$

An ODE is referred to as *component-wise monotonic* if it fulfills

$$s_i(q_i) (q_i^{\text{eq}} - q_i) > 0 \quad \forall q_i \neq q_i^{\text{eq}}. \quad (23)$$

The relaxation ODE under consideration in this work is of this type, and it is easy to verify that for such ODEs the backward Euler scheme will be stable in the sense that the solution to (22) will not overshoot an equilibrium point (Aursand et al., 2010). However, it should be emphasized that obtaining this solution requires solving a non-linear system of equations (22) by an iterative scheme such as the Newton–Raphson method. Instabilities can still occur if the non-linear solver fails to correctly solve this system.

Asymptotic Integration. A popular approach towards solving stiff systems in the form (20) has been the use of exponential integrators (Hochbruck et al., 1998; Cox & Matthews, 2002). The basic idea is that one gets rid of stability restrictions on the time step by approximating the stiff component of the solution as an exponential function. Recently, exponential methods tailored for relaxation systems have been proposed (Aursand et al., 2010). The first order method, referred to as ASY1, is given by

$$q_i^{n+1} = q_i^* + (q_i^{\text{eq}} - q_i^*) \left[1 - \exp\left(-\frac{\Delta t}{\tau_i}\right) \right], \quad (24)$$

where \mathbf{q}^{eq} is the equilibrium state and

$$\tau_i = \frac{q_i^{\text{eq}} - q_i^*}{s_i(\mathbf{q}^*)}. \quad (25)$$

The scheme (24)–(25) is unconditionally stable by construction—the numerical solution will decay exponentially to the equilibrium solution. However, the scheme requires a priori knowledge of the equilibrium state. The trade-off when using the ASY1 scheme as opposed to the Backward Euler scheme, is solving an equilibrium problem instead of an implicit numerical discretization. Depending on the system, calculating the equilibrium state \mathbf{q}^{eq} corresponding to an initial state \mathbf{q} can be either

trivial or very cumbersome. In the following, it will be discussed how to calculate the equilibrium state for the system (1)–(4).

When mass is moved from one phase to the other, total mass and energy are always conserved, as seen from Eq. (4), and by adding Eqs. (1) and (2). Thus, to calculate the equilibrium state for the mass transfer process, one needs to find the pressure p and temperature T as functions of the mixture density ρ and internal energy $E_{\text{int}} = \alpha_g \rho_g e_g + \alpha_\ell \rho_\ell e_\ell$, such that $\mu_g = \mu_\ell$. This corresponds to finding the boiling point for the given mixture density and internal energy.

In order to accomplish this, two nested Newton–Raphson algorithms were used. The algorithm may be briefly summarized as follows:

1. Guess a pressure p .
2. Find boiling point T_{boil} by solving $f_1(T_{\text{boil}}) = \mu_g(p, T_{\text{boil}}) - \mu_\ell(p, T_{\text{boil}}) = 0$ using the Newton–Raphson method,

$$T_{\text{boil}}^{n+1} = T_{\text{boil}}^n - \frac{f_1(T_{\text{boil}})}{f_1'(T_{\text{boil}})}. \quad (26)$$

For stiffened gas, the relevant expressions are then found from Eqs. (8) and (10),

$$\mu_k(p, T) = \gamma_k c_{v,k} T + e_{*,k} - c_{v,k} T \ln \left(\frac{T}{T_{0,k}} \left(\frac{\rho_{0,k} (\gamma_k - 1) c_{v,k} T}{p + p_{\infty,k}} \right)^{\gamma_k - 1} \right) - s_{0,k} T, \quad (27)$$

$$\left(\frac{\partial \mu_k}{\partial T} \right)_p = \frac{\mu_k - e_{*,k}}{T} - \gamma_k c_{v,k}, \quad (28)$$

where the subscript k denotes a quantity of phase k .

3. Solve

$$f_2(p) = \rho_g (\rho - \rho_\ell) e_g + \rho_\ell (\rho_g - \rho) e_\ell - (\rho_g - \rho_\ell) E_{\text{int}} = 0$$

for pressure p using a Newton–Raphson method, evaluated at $T = T_{\text{boil}}$. The method requires the derivative of f_2 , which for stiffened gas is given by

$$\begin{aligned} \frac{\partial f_2}{\partial p} = & ((\rho - \rho_\ell) e_g + \rho_\ell e_\ell + \frac{p}{\rho_g} (\rho - \rho_\ell) - E) \left(-\frac{\rho_g}{T} \frac{\rho_\ell - \rho_g}{\rho_g \rho_\ell (s_g - s_\ell)} + \frac{1}{c_{v,g} T (\gamma_g - 1)} \right) \\ & - ((\rho - \rho_g) e_\ell + \rho_g e_g + \frac{p}{\rho_\ell} (\rho - \rho_g) - E) \left(-\frac{\rho_\ell}{T} \frac{\rho_\ell - \rho_g}{\rho_g \rho_\ell (s_g - s_\ell)} + \frac{1}{c_{v,\ell} T (\gamma_\ell - 1)} \right) \\ & + \rho_g (\rho - \rho_\ell) \left(\gamma c_{v,g} \frac{\rho_\ell - \rho_g}{\rho_g \rho_\ell (s_g - s_\ell)} \right) \\ & - \rho_\ell (\rho - \rho_g) \left(\gamma c_{v,\ell} \frac{\rho_\ell - \rho_g}{\rho_g \rho_\ell (s_g - s_\ell)} \right) + (\rho_g - \rho_\ell), \end{aligned} \quad (29)$$

where $s_k = \frac{1}{T} (e + \frac{p}{\rho} - \mu)$ is the entropy of phase k .

4. Go to step 2 until $\mu_g - \mu_\ell$ is less than some chosen error limit.

For the present model, both the Backward Euler and ASY1 schemes require solving an iterative problem in each computational step. The relative stability and efficiency of these two schemes thus hinge on the stability and efficiency obtainable in their respective iterative schemes.

Numerical results

This section will present results for depressurization of a pipe with pure CO₂. The pipe has a length of $L = 100$ m, but for the sake of clearer plots, only the part $x \in [0, 80]$ will be shown. It is initially filled with liquid CO₂ at a pressure of $p = 60$ bar in the left part ($x \leq 50$ m) and gas at 10 bar in the right part ($x > 50$ m). The parameters used for the stiffened gas equation of state are shown in Table 1. The CFL number used was $C = 0.5$, while the initial volume fraction was $\delta = 0.01$. This case was also used by Lund and Aursand (2012), but in the present paper more focus is put on the results of different numerical methods.

Table 1: Stiffened gas parameters used in the simulation.

Phase	γ (-)	p_∞ (Pa)	c_v (J/kg K)	e_* (J/kg)	s_0 (J/kg K)	ρ_0 (kg/m ³)	T_0 (K)
Gas	1.06	$8.86 \cdot 10^5$	$2.41 \cdot 10^3$	$-3.01 \cdot 10^5$	$1.78 \cdot 10^3$	135	283.13
Liquid	1.23	$1.32 \cdot 10^8$	$2.44 \cdot 10^3$	$-6.23 \cdot 10^5$	$1.09 \cdot 10^3$	861	283.13

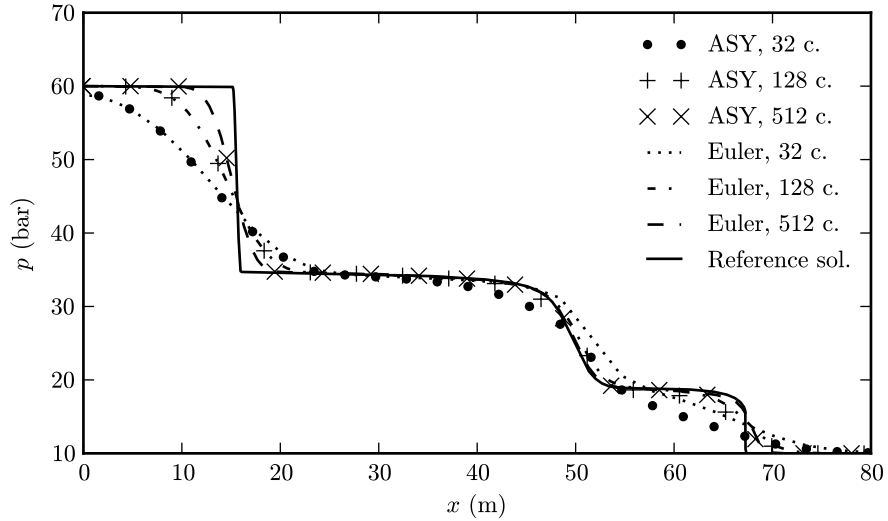


Figure 2. Pressure at time $t = 0.08$ s.

As time progresses, pressure waves will propagate to the left and right through the liquid and gas, respectively. Between these two pressure fronts, phase transfer in the form of evaporation and condensation will take place. Figure 2 shows the pressure after time $t = 0.08$ s, comparing the solutions using the ASY1 method and the Backward Euler method to a reference solution. The reference solution was obtained using a second order method and a very fine grid. In this reference solution, to the left of the front at $x \approx 16$ m, there is pure liquid, while there is pure gas to the right of $x \approx 55$ m.

From Figure 2, one can see that the two methods have very similar results with equal grid size. In the right part of the plot, we see that ASY1 is slightly more diffusive than the Backward Euler method with 32 grid cells. This difference between the two methods is perhaps even clearer in Figure 3, which shows the temperature for the same case. The temperature dip around $x \approx 55$ m is seen to be much clearer with the Backward Euler method than the ASY1 method, especially with the coarsest grids.

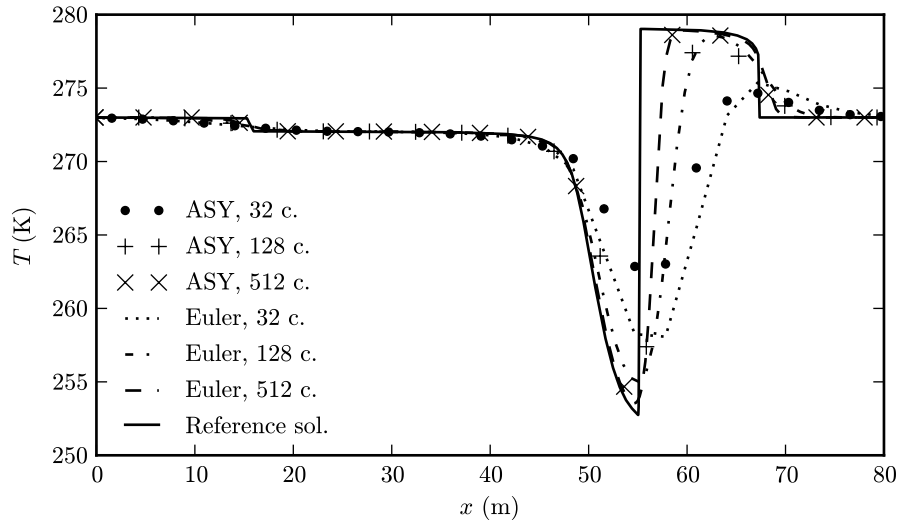


Figure 3. Temperature at time $t = 0.08$ s.

Finally, Figure 4 shows the volume fraction at the same time. One can notice that the dip in temperature seen in Figure 3 coincides with the abrupt change in volume fraction. To the left of this point, temperature drops due to evaporation of the liquid. Since the central MUSTA scheme was used, one can not expect such discontinuities to be properly resolved on coarse grids. A Roe solver is often more suitable for cases where discontinuities are dominant. Morin et al. (2009) has developed a Roe scheme for an equation system in the form presented in Eqs. (1)–(4), in the homogeneous case where $\Gamma = 0$.

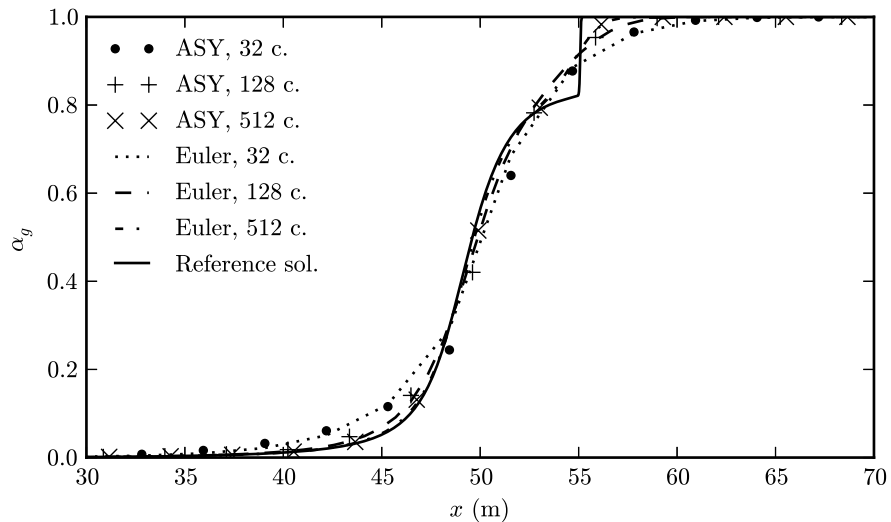


Figure 4. Gas volume fraction at time $t = 0.08$ s. Note: The graph only shows a part of the domain, $x \in [30, 70]$.

Table 2 shows the computational time spent for a range of different grid sizes, to give an impression of how the computational cost for the two methods are related. As seen in this table, the time

spent is rather similar for the same grid size, although the ASY1 scheme seems to have slightly better performance. It can be noted that the computational cost for the ASY1 method comes from calculating the equilibrium state, while the cost in the Backward Euler method is due to a Newton–Raphson iteration in the numeric scheme (22) itself. The cost for these two approaches may vary with different formulations of the source term than the one we have presented here, as it in some cases is possible to calculate the equilibrium state relatively cheap, in which case the ASY1 scheme would be expected to outperform the Backward Euler scheme.

Table 2: Computational time (in seconds) on a single Intel Core2 at 2.8 GHz for a range of different grid sizes.

Grid size	ASY1	Euler
512	6.23	7.15
1024	24.45	27.78
2048	99.26	110.71
4096	389.56	442.50

In the present case, the equation $\mu_g = \mu_\ell$ must be solved to find the equilibrium state, which has to be done numerically due to logarithms in the expression for μ , see Eq. (27). Say, for example, that the relaxation process in question was instead a heat transfer process, where the equilibrium state is given by $T_g = T_\ell$. This equation could, at least for the stiffened gas equation of state, be solved exactly without the use of a numerical scheme, thus decreasing the computational cost of the ASY1 scheme. Therefore one can expect the ASY1 scheme to have advantages over the Backward Euler method for other cases than the one presented here. However, for the present case, there does not seem to be any reasons to prefer one in front of the other, since the methods produce similar results at similar computational cost.

A final point worth making, is that the presented method is able to handle regions with volume fractions α_k of exactly zero. For other numerical methods found in the literature, it is often necessary to have non-zero volume fractions to avoid numerical instabilities (Munkejord et al., 2009; Chang & Liou, 2007). Chang and Liou (2007) report that numerical errors may be amplified when one phase disappears, leading to instabilities. The present approach has not shown to exhibit any issues related to a vanishing volume fraction.

Conclusion

A two-phase flow model has been presented, with phase transfer modelled using a relaxation term based on statistical rate theory. This model was solved using a first-order Godunov splitting scheme, making it possible to solve the hyperbolic equation system and the phase transfer model separately. The homogeneous hyperbolic equation system was solved using a central MUSTA scheme. Results for two different approaches to solving the phase transfer numerically were presented, one based on the Backward Euler method and one on the time-asymptotic ASY1 scheme. The ASY1 scheme has the advantage of being explicit if only the equilibrium state is known. However, with the particular model considered here, calculating the equilibrium state is done iteratively, which gives the ASY1 method similar performance to the Backward Euler method when it comes to accuracy and computational cost. In future work, one could apply the scheme to cases with an easier to compute equilibrium value, as well as investigate whether a second-order splitting scheme is beneficial when solving models similar to the one presented here.

Acknowledgement

This work was financed through the CO2 Dynamics project. The authors acknowledge the support from the Research Council of Norway (189978), Gassco AS, Statoil Petroleum AS and Vattenfall AB.

The authors would also like to thank Svend Tollak Munkejord, Bernhard Müller and Tore Flåtten for their useful comments.

References

- Aursand, P., Evje, S., Flåtten, T., Giljarhus, K. E. T., & Munkejord, S. T. (2010). An exponential time-differencing method for monotonic relaxation systems. *Preprint*. (Available at <http://www.math.ntnu.no/conservation/2011/008.pdf>)
- Azizian, S., Bashiri, H., & Iloukhani, H. (2008). Statistical rate theory approach to kinetics of competitive adsorption at the solid/solution interface. *Journal of Physical Chemistry C*, *112*(27), 10251-10255. Available from <http://pubs.acs.org/doi/abs/10.1021/jp802278e>
- Bordi, F., Cametti, C., & Motta, A. (2000). Ion permeation across model lipid membranes: A kinetic approach. *The Journal of Physical Chemistry B*, *104*(22), 5318-5323. Available from <http://pubs.acs.org/doi/abs/10.1021/jp000005i>
- Chang, C.-H., & Liou, M.-S. (2007). A robust and accurate approach to computing compressible multiphase flow: Stratified flow model and AUSM+-up scheme. *Journal of Computational Physics*, *225*(1), 840–873.
- Cox, S. M., & Matthews, P. P. (2002). Exponential time differencing for stiff systems. *J. Comput. Phys.*, *176*, 430-455.
- Dejmek, M., & Ward, C. A. (1998). A statistical rate theory study of interface concentration during crystal growth or dissolution. *The Journal of Chemical Physics*, *108*(20), 8698-8704. Available from <http://link.aip.org/link/?JCP/108/8698/1>
- Elliott, J. A. W., & Ward, C. A. (1997a, Apr 1). Statistical rate theory description of beam-dosing adsorption kinetics [Article]. *Journal of Chemical Physics*, *106*(13), 5667-5676.
- Elliott, J. A. W., & Ward, C. A. (1997b). Temperature programmed desorption: A statistical rate theory approach. *The Journal of Chemical Physics*, *106*(13), 5677-5684. Available from <http://link.aip.org/link/?JCP/106/5677/1>
- Findlay, R. D., & Ward, C. A. (1982). Statistical rate theory of interfacial transport. IV. Predicted rate of dissociative adsorption [Article]. *Journal of Chemical Physics*, *76*(11), 5624-5631.
- Flåtten, T., Morin, A., & Munkejord, S. T. (2010, Sep). Wave propagation in multicomponent flow models. *SIAM Journal on Applied Mathematics*, *70*(8), 2861-2882.
- Harding, L. B., Maergoiz, A. I., Troe, J., & Ushakov, V. G. (2000, Dec 22). Statistical rate theory for the $\text{HO} + \text{O} \rightleftharpoons \text{HO}_2 \rightleftharpoons \text{H} + \text{O}_2$ reaction system: SACM/CT calculations between 0 and 5000 K [Review]. *Journal of Chemical Physics*, *113*(24), 11019-11034.
- Hochbruck, M., Lubich, C., & Selhofer, H. (1998). Exponential integrators for large systems of differential equations. *SIAM J. Sci. Comput.*, *19*, 1552–1574.
- Jin, S. (1995). Runge–Kutta methods for hyperbolic systems with stiff relaxation terms. *J. Comput. Phys.*, *122*, 51-67.
- Kapoor, A., & Elliott, J. A. W. (2008, Nov 27). Nonideal Statistical Rate Theory Formulation To Predict Evaporation Rates from Equations of State [Article]. *Journal of Physical Chemistry B*, *112*(47), 15005-15013.
- LeVeque, R. J. (2002). *Finite volume methods for hyperbolic problems*. Cambridge University Press.
- Lund, H., & Aursand, P. (2012). Two-phase flow of CO₂ with phase transfer. *Energy Procedia*. (Accepted for publication, preprint available at <http://folk.ntnu.no/halvorlu>.)
- Menikoff, R., & Plohr, B. J. (1989). The Riemann problem for fluid flow of real materials. *Rev. Mod. Phys.*, *61*, 75-130.

- Morin, A., Aursand, P. K., Flåtten, T., & Munkejord, S. T. (2009, October 9-10). Numerical resolution of CO₂ transport dynamics. In *Siam conference on mathematics for industry: Challenges and frontiers (mi09)*. San Francisco, CA, USA.
- Munkejord, S. T., Evje, S., & Flåtten, T. (2006, October). The multi-stage centred-scheme approach applied to a drift-flux two-phase flow model. *International Journal for Numerical Methods in Fluids*, 52(6), 679-705.
- Munkejord, S. T., Evje, S., & Flåtten, T. (2009). A MUSTA scheme for a nonconservative two-fluid model. *SIAM J. Sci. Comput.*, 31(4), 2587-2622.
- Pao, Y.-P. (1971). Application of kinetic theory to the problem of evaporation and condensation. *Physics of Fluids*, 14(2), 306-312.
- Roe, P. L. (1981). Approximate Riemann solvers, parameter vectors, and difference schemes. *Journal of Computational Physics*, 43, 357-372.
- Rudzinski, W., & Plazinski, W. (2006, Aug 24). Kinetics of solute adsorption at solid/solution interfaces: A theoretical development of the empirical pseudo-first and pseudo-second order kinetic rate equations, based on applying the statistical rate theory of interfacial transport [Article]. *Journal of Physical Chemistry B*, 110(33), 16514-16525.
- Saurel, R., Petitpas, F., & Abgrall, R. (2008). Modelling phase transition in metastable liquids: application to cavitating and flashing flows. *Journal of Fluid Mechanics*, 607, 313-350.
- Stewart, H. B., & Wendroff, B. (1984). Two-phase flow: Models and methods. *Journal of Computational Physics*, 56, 363-409.
- Strang, G. (1968). On the construction and comparison of difference schemes. *SIAM J. Numer. Anal.*, 5, 506-517.
- Titarev, V. A., & Toro, E. F. (2005). MUSTA schemes for multi-dimensional hyperbolic systems: analysis and improvements. *International Journal for Numerical Methods in Fluids*, 49, 117-147.
- Toro, E. F. (1999). *Riemann solvers and numerical methods for fluid dynamics* (second edition ed.). Berlin: Springer-Verlag. (ISBN 3-540-65966-8)
- Toro, E. F. (2003, 17th June). *Multi-stage predictor-corrector fluxes for hyperbolic equations* (Technical Report No. NI03037-NPA). UK: Isaac Newton Institute for Mathematical Sciences, University of Cambridge.
- Ward, C. A., & Fang, G. (1999, Jan). Expression for predicting liquid evaporation flux: Statistical rate theory approach. *Phys. Rev. E*, 59(1), 429-440.
- Ward, C. A., Findlay, R. D., & Rizk, M. (1982). Statistical rate theory of interfacial transport. I. Theoretical development. *The Journal of Chemical Physics*, 76(11), 5599-5605.
- Ward, C. A., & Stanga, D. (2001). Interfacial conditions during evaporation or condensation of water. *Phys Rev E*, 64, 051509.